

Supporting Information

Impacts of Iron Rust Particle and Weak Alkalinity on Surfactant Micelle Structure and Drag Reduction Ability

Na Xu^{a, b}, Zilu Liu^a, Fei Liu^c, *^{*}, Wei Hong^c

^aCollege of Chemical Engineering and Technology, Taiyuan University of Technology, Taiyuan,
030024, P. R. China

^bShanxi Coking Coal in Yuncheng Salt Refco Group Ltd., Yuncheng, 044000, P. R. China

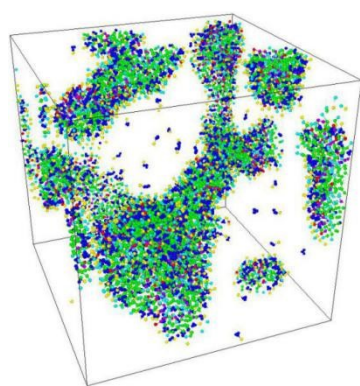
^cShenzhen Key Laboratory of Soft Mechanics & Smart Manufacturing, Department of
Mechanics and Aerospace Engineering, Southern University of Science and Technology,
Shenzhen, 518055, P. R. China

*To the correspondence should be addressed. E-mail: liuf@sustech.edu.cn. Telephone: +86-
755-88018182 (L.F.).

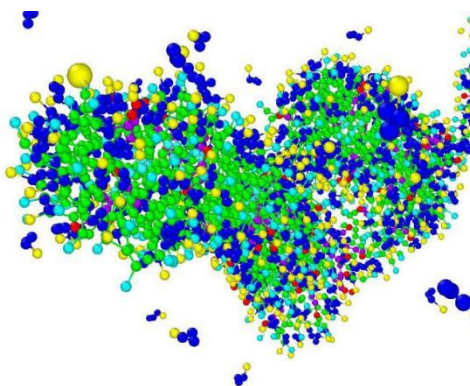
Table S1: The non-bonded parameters for CTAC, nanoparticles, NaSal and water in the MARTINI force field.

Site 1	Site 2	ε_{ij} (kJ·mol ⁻¹)	σ_{ij} (nm)
Qa	Qa	5.0	0.47
Qa	Q0	4.5	0.47
Qa	C2	2.0	0.62
Qa	C1	2.0	0.62
Qa	SC4	2.7	0.43
Qa	Qd	5.6	0.47
Qa	P4	5.6	0.47
Qa	BP4	5.6	0.47
Q0	Q0	3.5	0.47
Q0	C2	2.0	0.62
Q0	C1	2.0	0.62
Q0	SC4	2.7	0.47
Q0	Qd	4.5	0.47
Q0	P4	5.6	0.47
Q0	BP4	5.6	0.47
C2	C2	3.5	0.47
C2	C1	3.5	0.47
C2	SC4	3.1	0.47
C2	Qd	2.0	0.62
C2	P4	2.3	0.47
C2	BP4	2.3	0.47
C1	C1	3.5	0.47
C1	SC4	3.1	0.47

C1	Qd	2.0	0.62
C1	P4	2.0	0.47
C1	BP4	2.0	0.47
SC2	SC4	3.1	0.43
SC2	Qd	2.0	0.62
SC2	P4	2.3	0.47
SC2	BP4	2.3	0.47
SC4	SC4	2.6	0.43
SC4	Qd	2.7	0.47
SC4	P4	2.7	0.47
SC4	BP4	2.7	0.47
Qd	Qd	5.0	0.47
Qd	P4	5.6	0.47
Qd	BP4	5.6	0.47
P4	P4	5.0	0.47
P4	BP4	5.0	0.57
BP4	BP4	5.0	0.47



(a)



(b)

Figure S1. (a) A global perspective of the surfactant micells in the weak alkalinity solution. (b) Detailed morphology of a surfactant micelle in the weak alkalinity solution. Simulation conditions: The simulation box is $27 \text{ nm} \times 27 \text{ nm} \times 27 \text{ nm}$; $C_{\text{CTA}^+} = 0.20 \text{ mol}\cdot\text{L}^{-1}$, $C_{\text{Sal}^-} = 0.20 \text{ mol}\cdot\text{L}^{-1}$, $T = 300 \text{ K}$; The ratio of the modified CTA^+ (existing in weakly alkaline solution) to the normal CTA^+ (existing in neutral solution) is set to 1:1; Cl^- and water CG sites are hidden.

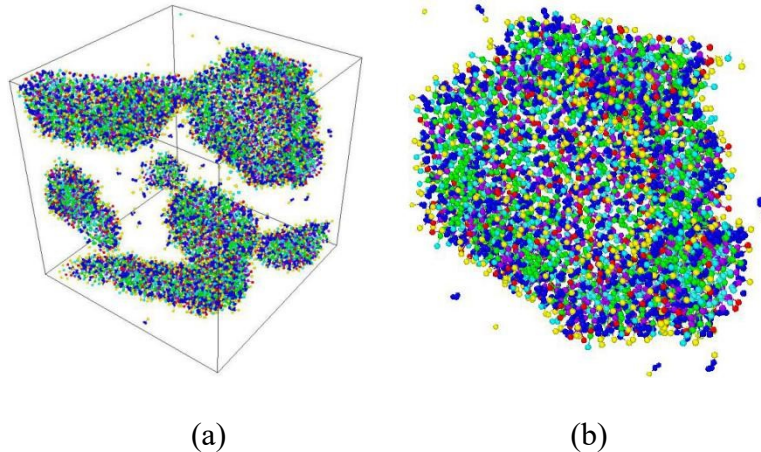


Figure S2. (a) A global perspective of the surfactant micells in the weak alkalinity solution. (b) A pie-like surfactant micelle in the weak alkalinity solution. Simulation conditions: The simulation box is $27 \text{ nm} \times 27 \text{ nm} \times 27 \text{ nm}$; $C_{\text{CTA}^+} = 0.40 \text{ mol}\cdot\text{L}^{-1}$, $C_{\text{Sal}^-} = 0.40 \text{ mol}\cdot\text{L}^{-1}$, $T = 300 \text{ K}$; The ratio of the modified CTA^+ (existing in weakly alkaline solution) to the normal CTA^+ (existing in neutral solution) is set to 1:1; Cl^- and water CG sites are hidden.

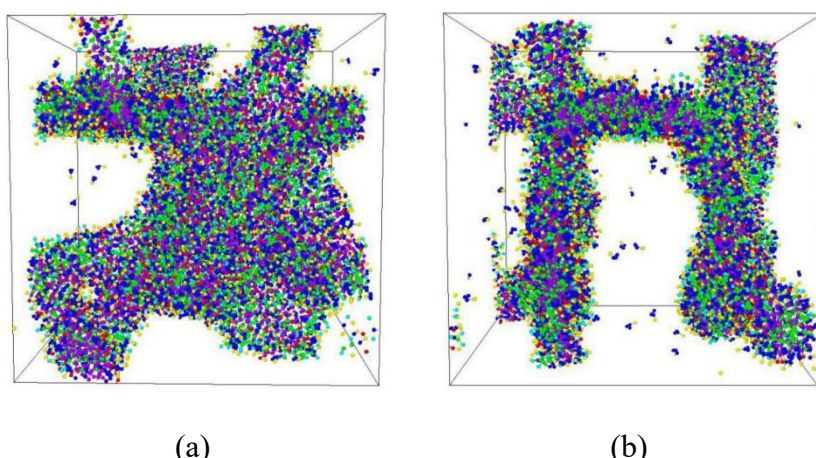


Figure S3. (a) A global perspective of the surfactant micells in the weak alkalinity solution. (b) A bridge-like surfactant micelle in the weak alkalinity solution. Simulation conditions: The

simulation box is $27 \text{ nm} \times 27 \text{ nm} \times 27 \text{ nm}$; $C_{\text{CTA}^+} = 0.50 \text{ mol}\cdot\text{L}^{-1}$, $C_{\text{Sal}^-} = 0.50 \text{ mol}\cdot\text{L}^{-1}$, $T = 300 \text{ K}$; The ratio of the modified CTA^+ (existing in weakly alkaline solution) to the normal CTA^+ (existing in neutral solution) is set to 1:1; Cl^- and water CG sites are hidden.